

# Mesenchymal Stem Cells Versus Their Conditioned Medium for Managing Systemic Sclerosis Associated Arthritis Rat Model: Histological and Immunohistochemical Study

Amira Adly Kassab<sup>1,2</sup>, Ahmed A. A. Abd-El-Hafez<sup>3</sup>, Ali El-Deeb<sup>4</sup> and Amal A. A. Abd-El-Hafez<sup>1</sup>

## Original Article

<sup>1</sup>Department of Histology, Faculty of Medicine, Tanta University, Egypt

<sup>2</sup>Department of Basic Medical Sciences, Faculty of Medicine, Ibn Sina University for Medical Sciences, Jordan

<sup>3</sup>Department of Anesthesia, Surgical ICU and Pain Management, Faculty of Medicine, Tanta University, Egypt

<sup>4</sup>Department of Rheumatology and Rehabilitation, Faculty of Medicine, Tanta University, Egypt

## ABSTRACT

**Introduction:** Systemic sclerosis (SS) is an autoimmune disorder with high morbidity. It is characterized by chronic inflammation and fibrosis. The articular manifestations of SS were reported in many cases.

**Aim of the Work:** To explore novel mechanisms involved in systemic sclerosis associated arthritis and to compare the therapeutic effects of the mesenchymal stem cells (BM-MS) versus their conditioned medium (MS-C) on knee joint arthritis associated in a model of systemic sclerosis in rats.

**Materials and Methods:** Forty rats were divided into group I (Control), group II (SS-associated arthritis) and group III (Treated group). Group III was further arranged into subgroup III-a (BM-MS treated group) and subgroup III-b (MS-C treated group). Four weeks from the last injection in all subgroups, excision of the entire knee joints was done to be processed for the histological and immunohistochemical study.

**Results:** Group II revealed disturbed histological structure of the articular cartilage, subchondral bone and synovium. Surface irregularities, clefts and superficial erosion of the cartilage were noticed. Degenerated subchondral bone matrix was observed. The synovial membrane showed vascular congestion, edema and inflammatory cellular infiltration. Moreover, there was a significant decrease in the articular cartilage and subchondral bone thickness and in collagen content of the matrix of the articular cartilage. The synovial membrane showed marked subintimal collagen deposition and a significant increase in the immuno-expression of urokinase plasminogen activator (UPA). In contrast, group III showed improvement of all above mentioned parameters which were highly marked in subgroup III-b comparing to subgroup III-a.

**Conclusion:** MS-C had better therapeutic effects on SS-associated knee arthritis than BM-MS.

**Received:** 03 September 2022, **Accepted:** 14 September 2022

**Key Words:** Arthritis, conditioned medium, mesenchymal stem cells, rat model, systemic sclerosis.

**Corresponding Author:** Amira Adly kassab, MD, Department of Basic Medical Sciences, Faculty of Medicine, Ibn Sina University for Medical Sciences, Amman 16197, Jordan, **Tel.:** +20 10 1669 7635, **E-mail:** Amirakassab80@yahoo.com / amirakassab@isums.edu.jo

**ISSN:** 1110-0559, Vol. 46, No. 4

## INTRODUCTION

Systemic sclerosis (SS) is a chronic connective tissue disorder which is autoimmune mediated. Although it is a rare, it possesses high morbidity and mortality. It is characterized by vasculopathy, chronic inflammation and tissue fibrosis and atrophy<sup>[1,2]</sup>. The underlying etiology is unknown. The pathogenesis of SS may involve genetic as well as environmental factors that induce SS-specific genes in various cells resulting in the characteristic pathological and clinical manifestations<sup>[3,4]</sup>. Many cytokines are also taking part in its pathogenesis as the proinflammatory IL-6

and the fibrosis related IL-13 in addition to the transforming growth factor<sup>[5,6]</sup>.

There are two types for SS according to the spread of the sclerotic skin area; diffuse and limited cutaneous SS. In both types, fibrotic changes occur in the visceral organs as lungs and esophagus. Patients suffering from this disorder are positive for anti-RNA polymerase III antibody, anti-topoisomerase-1 antibody and anti-centromere antibody. The early clinical manifestation of SS is Raynaud's phenomenon due to cold stimulus followed by swollen edematous fingers with gradual hardening of the skin.

This leads to limited joint movement and reduced daily activity<sup>[5,7]</sup>.

Musculoskeletal manifestations in SS were also reported which vary from arthralgia to arthritis. Muscles may be also affected, and patients suffer from muscle pain, atrophy and weakness. In addition, calcinosis as well as tendon friction rubs due to tendon sheath inflammation and fibrosis may occur. Hand arthritis, synovitis, joint erosions, skin thickening with flexion contracture and limited hand motion may be early symptoms with Raynaud's phenomenon. The radiological studies on SS showed remarkable joint abnormality as erosions, narrowing and arthritis in addition to bone changes as demineralization, bone resorption and acro-osteolysis<sup>[8,9,10,11]</sup>.

Bleomycin is an antitumor agent that is commonly used in many therapeutic regimens. Bleomycin-induced SS model in animals is widely applied to study different aspects and pathogenesis of the disease in addition to evaluation of new antifibrotic therapies. Bleomycin can induce skin fibrosis, systemic inflammation and autoimmune response as found in SS disorder<sup>[12]</sup>.

In the last few years, mesenchymal stem cells (MS) are easily isolated, cultured and applied for tissue regeneration. They have a therapeutic action in many disorders and can improve tissue fibrosis<sup>[13]</sup>.

The cell-based therapy for cartilage repair was researched since 1980s. Nowadays, mesenchymal stem cells are considered as a main therapeutic tool in osteoarthritis because of their ability to differentiate into chondrocytes in addition to their immunomodulatory properties helping in cartilage regeneration. Moreover, MS may play a role in reducing the inflammation by homing into inflamed tissues, regulating immune and inflammatory responses, thus facilitating the repair process. MS possesses immunosuppressive effects as they can inhibit T-lymphocyte activation and proliferation, thus modulating the expression of pro-inflammatory cytokines<sup>[14,15]</sup>.

Recently, it was proved that the regenerative capacity of MS can be primarily mediated by paracrine factors (secretomes). These factors are secreted by MS in their medium, thus this medium is known as conditioned medium<sup>[16]</sup>. The secretomes of conditioned medium have several advantages over MS as low immunogenicity and oncogenic effect. They have ability to cross the biological membrane. So, extensive studies on MS-derived secretomes are currently underway to be used as an alternative to MS or an effective cell-free therapy<sup>[17]</sup>.

Conditioned media of MS (MS-C) contain growth factors and cytokines that help in tissue repair. MS-C contain also extracellular vesicles as exosomes, microvesicles and apoptotic bodies<sup>[18]</sup>. Initially, extracellular vesicles are considered as a waste of cell damage or a by-product of cell homeostasis with no significance. Recently, it was reported that these vesicles are functional because they carry bioactive compounds. These bioactive compounds are cell-

specific proteins and lipids in addition to genetic materials that can be taken up by neighboring and distant cells for reprogramming of these recipient cells. So, extracellular vesicles may have a role in the cellular processes as the immune response and chronic inflammation through the intercellular communication<sup>[19]</sup>.

Mesenchymal stem cells derived secretomes exerted main effects on tissue regeneration as cartilage repair in articular cartilage diseases<sup>[20]</sup>. Their therapeutic capacity has been tested in many studies and showed a therapeutic effect which is comparable to MS themselves<sup>[21,22]</sup>.

## AIM OF THE WORK

This histological study was performed to explore novel mechanisms involved in systemic sclerosis associated arthritis and to compare the therapeutic effects of the bone marrow derived mesenchymal stem cells (BM-MS) and their conditioned medium (MS-C) on knee joint arthritis associated with bleomycin induced model of systemic sclerosis in adult male albino rats.

## MATERIALS AND METHODS

### *Ethical approval*

The animal work was performed by application of guidelines for animal research approved by the Research Ethics Committee of Faculty of Medicine; Tanta University; Egypt (Approval code: 35104/12/21).

### *Chemicals*

- Bleomycin ampoules (15 mg) were from Nippon Kayaku Co., Japan, Cat. No; 971.
- Roswell Park Memorial Institute (RPMI) 1640 medium (500 ml) was from Lonza Co., Swiss, Cat. No; BE12-702F.
- Fetal bovine serum (FBS) was from Gibco, Invitrogen Co., Austria, Cat. No; A11-151.
- Antibiotic-Antimycotic (Penicillin-Streptomycin-Amphotericin-B Mixture) was from Lonza CO., Switzerland, Cat. No; 17-745 E.
- Phosphate Buffered Saline (PBS) was from Lonza Bioproduct, Switzerland Cat. No; BE 17-512 F.
- Trypsin/EDTA solution was from Lonza Co., Cat. No; BE 17-161E.

### *The used protocol for establishing BM-MS culture*<sup>[23]</sup>

The protocol was done at the Tissue Culture Unit of Histology Department, Faculty of Medicine, Tanta University. Rats of subgroup I-a were a source for BM-MS. Their tibias, femurs and humeri were dissected. Both ends of the bones were removed with sharp scissors. Bone marrow was flushed out into tissue culture dishes from the bone cavity using complete culture medium. The dish containing the extracted bone marrow was then incubated at 37°C in a 5% CO<sub>2</sub> incubator. Nonadherent cells were removed 24-72 hours later by changing the medium. The

extracted bone marrow was cultured for mesenchymal stem cells. This was passage 0 in the 1st day. When the cells (Passage 0) reached confluence (70- 80%) after about (7-9) days, subculture was done at a split ratio 1:3 to get passage 1 which upon getting confluence (70-80%), trypsinization was done to reach passage 2 which upon getting confluence (70-80%) trypsinization was done to get passage 3.

#### **a-Culture and expansion of MSCs**

The inverted microscope was used daily to assess the expansion of the cultured cells and to detect any fungal or bacterial infection. Nonadherent cells were removed three days after the primary culture by a sterile pipette. The adherent cells were washed with phosphate buffered saline twice. Then addition of 7 ml of the fresh culture media to each flask was done. Mesenchymal stem cells were distinguished from other bone marrow cells by their adherence to the plastic flasks. The culture medium was changed every 2days to remove the nonadherent cells. The second exchange of medium was done after 5 days when spindle shaped cells with long processes and vesicular nuclei were obtained.

#### **b-Trypsinization**

It was done using trypsin EDTA to do subculture. Repeating this process 3 times was done. Then cells of passage 3 were trypsinized, washed and suspended in phosphate buffered saline at a concentration of  $10^6$  /ml.

#### **c-Counting of the mesenchymal stem cells**

The total cell count and viability of the cells was determined by using the hemocytometer. Trypan blue 0.4% was applied for viable cell counting. Living cells do not take up the dye, but dead cells do. 0.5ml of cell suspension was mixed with 0.5ml of trypan blue suspension (0.4%). This 1:1 dilution of the cells and dye was allowed to stand for about 2 minutes then shaken well. All cells in the four 1 mm corner square were counted. In addition, the viable and non-viable cells were counted separately. The cell concentration was calculated as follows:

$$\text{Cells/ml} = \text{mean cell count per square} \times \text{dilution factor} (1) \times 10^4.$$

#### **d-Preparation of mesenchymal stem cell suspension**

The cells of passage 3 were used for intra articular injection. The sterile tube containing the cell suspension was exposed to centrifugation at 2000 rpm for 10min. The supernatant was removed carefully to obtain the cell pellet. The cell viability was performed by trypan blue and cell count was done using a hemocytometer. The total viable cells injected were  $2.5 \times 10^6$  / rat.

#### **Characterization of BM-MS by differentiation**

In order to characterize BM-MS, osteogenic, chondrogenic and adipogenic differentiation potential was induced by culturing confluent BM-MS cells in differentiation media for 3 weeks. Then, the cells were stained with 2% Alizarin red, Alcian blue, 2% oil red O for osteocytes, chondrocytes and adipocytes respectively.

For adipogenic differentiation, droplets of fat vacuoles were found. For chondrogenic differentiation, blue dots of glycosaminoglycans were found. For osteogenic differentiation, red calcium deposits were found in cells<sup>[24]</sup>. The procedures were performed at Unit of Biochemistry and Molecular Biology, Medical Biochemistry and Molecular Biology Department, Faculty of Medicine, Cairo university.

#### **Flow cytometry analysis**

To assess the immune activity of BM-MS, flow cytometry was used. Cells were stained with antibodies for CD34, CD45, CD105, CD90. Analysis of cells was performed on FACS flow cytometry using Cell Quest Software (Becton Dickinson, UK)<sup>[24]</sup>. The procedures were performed at Unit of Biochemistry and Molecular Biology, Medical Biochemistry and Molecular Biology Department, Faculty of Medicine, Cairo university.

#### **MS-C preparation**

The MS-C preparation was done from bone marrow derived mesenchymal stem cells (passage 3). MS were seeded in their culture medium overnight at a density of  $2.5 \times 10^6$  cells/ culture plate. Three washes with PBS were done and 30 ml of the medium (free of FBS) was added. Cells were cultured for 24 hours. Then, centrifugation was done (1000 rpm/10 minutes at 4°C). Then, supernatant was used as such for the injection<sup>[25]</sup>. The protocol was done at the Tissue Culture Unit of the Histology Department, Faculty of Medicine, Tanta University.

#### **Animals and Study design**

The study used 40 adult male albino rats, weighed 200-230 grams and aged 12-16 weeks from the animal house of Tanta Faculty of Medicine. The protocol was done at the Histology Department, Faculty of Medicine, Tanta University. Rats lived under similar conditions in hygienic ventilated stainless-steel coops and had a good supply of food and water throughout the experiment. For two weeks before the experiment, rats were acclimatized to the environment.

Two main groups of rats were designed:

##### **Group I (Control group):**

- Subgroup I-a: 10 rats didn't receive any medications for the histological study of the knee joint structure. Moreover, bone marrow of their humeri, femurs and tibias were cultured for BM-MS.
- Subgroup I-b: 10 rats were subcutaneously injected with 0.1ml saline [vehicle for bleomycin] daily for 4 weeks.

**Group II (SS-associated arthritis group):** 10 rats were subcutaneously injected with 0.1 mg bleomycin once daily for 4 consecutive weeks. The knee joints were obtained after 4 weeks from the last day of bleomycin injection<sup>[26]</sup>.

**Group III (Treated group):** It was formed of 10 rats. After dealing with bleomycin as in group II, the following procedures was done;

- The right knee joints of the 10 rats were injected (single intra-articular injection) with BM-MS ( $2.5 \times 10^6$ ) suspended in 0.5 ml fresh specific media (Subgroup III-a or BM-MS treated group)<sup>[23]</sup>.
- The left knee joints of the same rats were injected (single intra-articular injection) with 100  $\mu$ l of MS-C (Subgroup III-b or MS-C treated group)<sup>[16]</sup>.

For intra-articular injections, the animals were anesthetized, the hair of the knee joint was shaved and the skin was sterilized. On back position, the knee joint was flexed and immobilized. Then, the intra articular injection was done by using insulin syringe through the joint capsule<sup>[27]</sup>.

Four weeks from the last injection in all subgroups, the rats were anesthetized by sodium pentobarbital (50mg/Kg, intraperitoneal)<sup>[28]</sup>. Excision of the entire right and left knee joints was done to be processed for histological study.

### **Joint processing**

The joints were immediately fixed in 10% neutral-buffered formalin for 24 hours. Then, they were washed in tap water and were decalcified using disodium EDTA for 4 weeks until the tissue become soft<sup>[29]</sup>. After that, the decalcified joints were washed, dehydrated, cleared and paraffin immersed. Finally, sections were cut (five  $\mu$ m thickness) and stained with hematoxylin and eosin for general structure [H&E] and Masson's trichrome stains for collagen deposition<sup>[30]</sup>.

For immunohistochemical staining, five micrometer sections were dewaxed, rehydrated, and washed with phosphate buffered saline; PBS. The sections were incubated with a primary antibody for urokinase plasminogen activator (UPA) [Rabbit polyclonal anti-urokinase antibody, 1.0  $\mu$ g/ml, ab24121, Abcam, Cambridge, UK] overnight in a humid chamber at 4°C and then incubated for 60 minutes with biotinylated goat anti-rabbit IgG at room temperature. Sections were incubated with a streptavidin–biotin–horseradish peroxidase complex for another 60 minutes. The immunoreactivity was visualized by 3,3'-diaminobenzidine's chromogenic reaction. Sections were counterstained with Mayer's hematoxylin. The negative control sections were prepared by using PBS instead of the primary antibodies<sup>[31]</sup>. Positive control for UPA is prostate and prostate cancer. UPA immunoreactivity was localized in the blood vessels of synovium [in the endothelial and intravascular cells].

### **Morphometric study**

A Leica microscope coupled to a CCD camera was used to take the photos. Morphometrical evaluation of the images was performed by an image analysis image J program (revamped by US software developer Wayne Rasband at the National Institutes of Health, Public Domain, BSD-2), to measure the following parameters:

- Thickness of the articular cartilage of the femur in the central area in H&E stained slides (X400).
- Thickness of the subchondral bone plate of the femur in H&E stained slides (X400).
- Area percentage [area %] of collagen content of the articular cartilage matrix in Masson's trichrome stained slides (X400) in ten fields for each slide.
- Area percentage of collagen content of the subintima of the synovial membrane in Masson's trichrome stained slides (X400) in ten fields for each slide.
- Area percentage of the positive UPA immun-expression of synovium in DAB stained sections (X400) in ten fields for each slide.

### **Statistical analysis**

Statistical package for social sciences statistical analysis {SPSS Inc., version 11.5, USA} software was utilized for data analysis. The morphometric results were subjected to one-way analysis of variance as well as Tukey's procedure. The mean as well as standard deviation values for all parameters {Mean  $\pm$  SD} were calculated<sup>[32]</sup>.

## **RESULTS**

The experiment was performed with no complications after the intra-articular injections with zero mortality.

### **Morphological identification of BM-MS**

BM-MS exhibited fibroblast appearance with star or spindle shaped cell body, multiple interdigitating extensions and vesicular central nuclei. BM-MS showed confluence of 80%-90% (Figure A).

### **Functional characterization of BM-MS**

BM-MS were able to be differentiated into osteogenic, chondrogenic and adipogenic lineages. The differentiated cells to adipocytes showed positive oil red O staining with accumulated lipid vacuoles. The differentiated cells to chondrocytes expressed blue dots of aminoglycans by Alcian blue. The differentiated cells to osteocytes gave positive staining of calcium deposits by alizarin red (Figures B,C,D).

### **BM-MS surface markers expression**

BM-MS were positive for CD90 and CD105 and were negative for CD34 and CD45 (Figure E).

### **Light microscopic findings**

#### **H&E staining**

**Group I (Control group):** normal histological appearance of the knee joint tissue was found in this group. The knee joint tissue was formed of two articular cartilages, subchondral bone and synovium. The articular cartilages had smooth surfaces and normal columnar orientation of the chondrocytes with intact tide mark as well as subchondral bone (Figure 1). Four zones of the articular cartilage could be

identified; superficial tangential, intermediate transitional, deep radial and calcified cartilage zones. The superficial zone had elongated flat chondrocytes. The intermediate zone had rounded chondrocytes which were randomly distributed. The deep radial one had short columns of large round chondrocytes which were oriented perpendicular to the surface. The calcified zone had a few scattered small chondrocytes with apoptotic nuclei. The tide mark was a deep basophilic line which was present between the calcified zone and the uncalcified zones (Figure 2). Moreover, the subchondral bone was composed of a subchondral bone plate, and cancellous bone trabeculae with bone marrow spaces. A joint space could be seen having two wedges of the fibrocartilaginous menisci (Figure 1) and was lined with the synovial membrane except the articular cartilages and the menisci. The synovial membrane had numerous folds and was formed of intimal and subintimal layers. The intimal layer showed 1-2 cell rows (synoviocytes). The subintimal layer was loose connective tissue having blood vessels, fibroblasts and collagen fibers (Figure 3).

**Group II (SS-associated arthritis group):** The examination revealed affection of the histological structure of the articular cartilage of femur and tibia, their subchondral bones and synovial membrane. This group showed damage of the articular cartilage with apparent decrease in its thickness. Surface irregularities, clefts or superficial erosion were present in many areas. Moreover, some areas showed contact between the articular cartilage and bone marrow spaces. The calcified cartilage zone interdigitated with the trabecular bone. There were also areas of degenerated subchondral bone and bone marrow. Chondrocyte aggregation was observed. Bone marrow spaces were filled with inflammatory cells (Figures 4,5,6). Loss of the normal zonal arrangement and orientation of the chondrocytes was noticed (Figure 6). Narrowing of the joint space with focal adhesion of the two articular cartilages appeared in other specimens with invasion of bone marrow cells into the articular cartilage (Figure 7). The synovial membrane showed several cell rows of synoviocyte (hyperplasia), disappeared folds (Figure 8), vascular congestion, edema (Figure 9) and inflammatory cellular infiltration with proliferation of the synovium over the articular cartilage (Figure 10).

**Group III (Treated group):** Both right and left knee joints (subgroup III-a and III-b) showed improvement of the histological structure of the articular cartilage, subchondral bone and synovial membrane. This improvement was better in subgroup III-b than subgroup III-a. Subgroup III-a (BM-MS treated group) showed smooth articular surface with apparent increase in its thickness. However, focal areas showed some degenerated chondrocytes. Also, focal areas showed apparent thin subchondral bone. The synovial membrane appeared with its two cell layers of the intima with a few congested blood vessels, edema and mononuclear cellular infiltration of the subintima (Figures 11,12). Regarding subgroup III-b (MS-C treated group), marked improvement was noticed

in the articular cartilage, subchondral bone and also in the synovial membrane. The cartilage showed smooth surface with apparent normal thickness, normal zonal arrangement and columnar orientation of the chondrocytes with intact tide mark. Moreover, apparent thick areas of subchondral bone were observed. In addition, nearly normal histological appearance of the intima and subintima of the synovial membrane was detected in most specimens (Figures 13,14).

#### ***Masson trichrome staining***

The control group showed normal collagen fiber distribution in the uncalcified and calcified zones of the articular cartilage in addition to a few collagen fibers in the subintima of the synovial membrane (Figures 15,16). Group II showed marked apparent decrease in the collagen fibers of all zones of the articular cartilage with abundant subintimal collagen fibers deposition (Figures 17,18). Whereas, subgroup III-a and III-b revealed increased collagen fibers of all zones of the articular cartilage of the right and left knee joints associated with a moderate amount of collagen fibers in the subintima (Figures 19,20,21,22). However, a few areas in the hyaline cartilage of subgroup III-a (BM-MS treated group) appeared with reduced collagen content (Figure 19).

#### ***Immunohistochemistry for UPA***

Negative UPA immunoreactivity or a faint reaction was observed in the synovial membrane of the control group (Figure 23). Group II showed a strong UPA positive cytoplasmic immunoreactivity in the wall of blood vessels of the synovial membranes and in the intravascular cells (Figure 24). However, subgroup III-a and III-b expressed a very weak positive UPA reaction in sparse blood vessels of the synovium of the right and left Knee joints (Figures 25,26).

#### ***Statistical results of the morphometric measurements (Table 1)***

The mean thickness of the articular cartilage and subchondral bone plate in group II was significantly reduced compared to control, while subgroup III-a and III-b revealed a non-significant decrease compared to control (Histogram 1A,2).

The mean area percentage of collagen content of the articular cartilage matrix in group II showed a significant decrease when compared to control one, while subgroup III-a and III-b showed a non-significant decrease compared to control (Histogram 1B).

The mean area percentage of the subintima collagen content of the synovial membrane of group II showed a significant increase when compared to control one, while subgroup III-a and III-b showed a non-significant increase compared to control (Histogram 1C).

The mean area percentage of UPA immuno-expression of synovium in group II showed a significant increase when compared to control, while subgroup III-a and III-b

showed a non-significant increase compared to control (Histogram 1D).

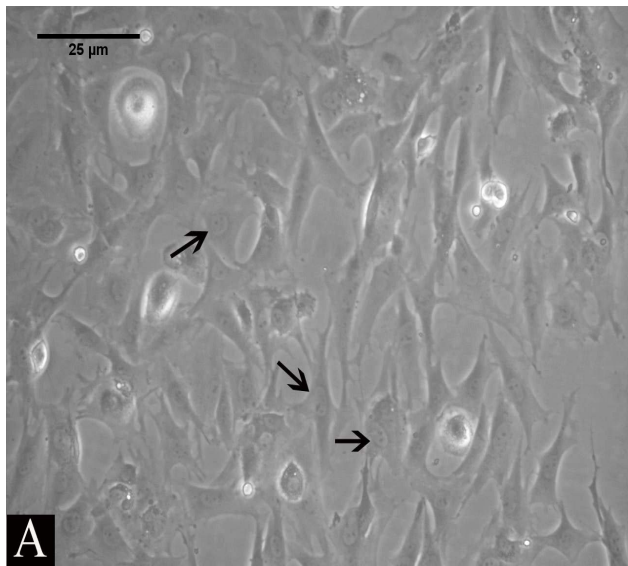


**Fig. A:** A phase contrast photomicrograph shows BM-MS morphology. Notice, spindle-shaped BM-MS with many processes and central vesicular nuclei. Cultured cells show 80%-90% confluence. (Inverted Microscope, X 400)

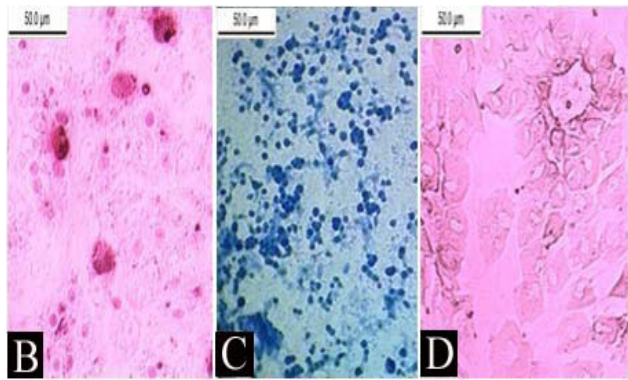


**Fig. B,C,D:** Tri-lineage differentiation potential of BM-MS. B) Differentiation into osteocytes. C) Differentiation into chondrocytes. D) Differentiation into adipocytes. ((B)Alizarin Red, (C)Alcian Blue, (D)Oil Red O, X400)

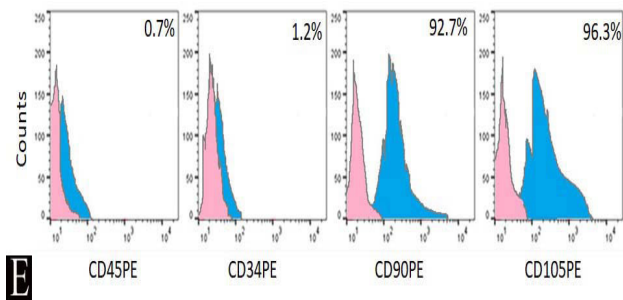


**Fig. E:** Flow cytometry analysis of BM-MS surface markers. Positive expression of BM-MS surface markers (CD90 and CD105) and negative expression of hematopoietic markers (CD34 and CD45).

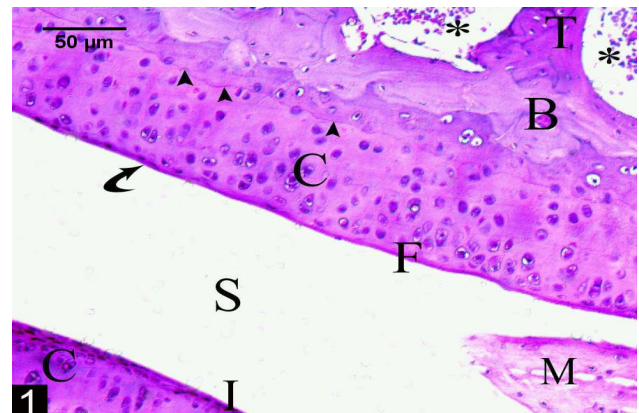


**Fig. 1:** A photomicrograph of a rat knee joint from group I (control) showing two articular cartilages (C) of femur (F) and tibia (I) having smooth surfaces (curved arrow) separated by a wide space (S). The tide mark is a prominent basophilic line (arrow head) in the cartilage. Notice the subchondral bone plate (B), trabecular bone (T) and bone marrow spaces (\*). The fibrocartilaginous meniscus projects into the joint space (M). (H&E, X200)

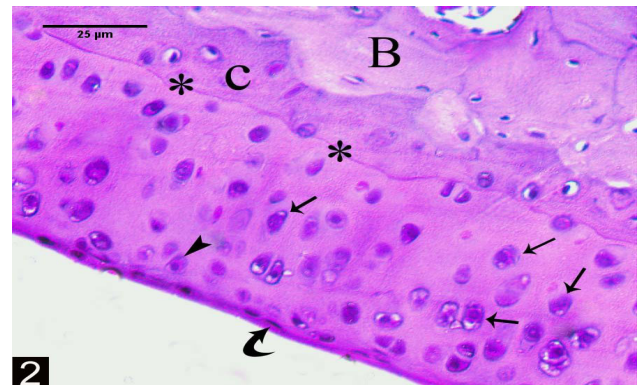


**Fig. 2:** A photomicrograph of the articular cartilage of the rat knee joint from group I showing its four zones; superficial zone containing flat chondrocytes (curved arrow), intermediate zone containing small round chondrocytes (arrow head), deep radial zone containing large chondrocytes (arrow) and calcified cartilage zone containing chondrocytes with apoptotic nuclei (C). Notice, the underlying bone plate (B) and the dark basophilic tide mark (\*) separating the calcified from uncalcified zone.(H&E, X400)

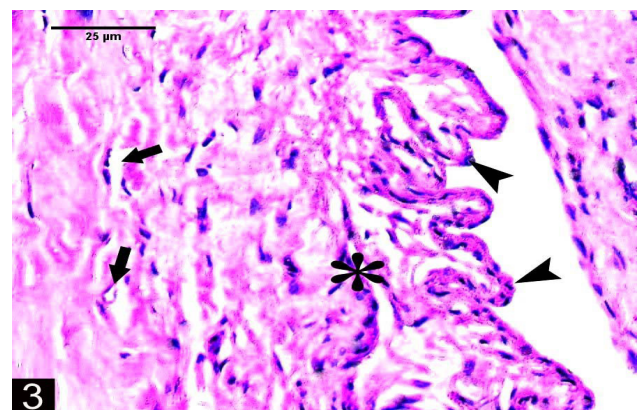


**Fig. 3:** A photomicrograph of the synovial membrane of the rat knee joint from group I showing one cell layer of the intima with numerous folds (arrow head) and subintimal layer of connective tissue containing fibroblasts, collagen fibers (\*) and blood vessels (arrow).(H&E, X400)

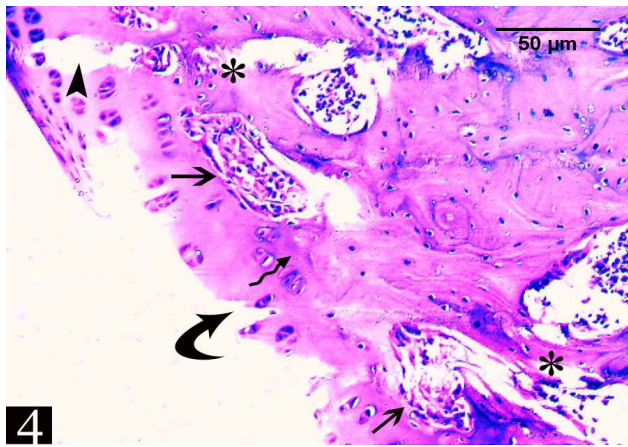


**Fig. 4:** A photomicrograph of the articular cartilage of the rat knee joint from group II showing surface erosion (curved arrow) and cleft (arrow head). Notice the contact between the articular cartilage and bone marrow spaces (arrow). The calcified cartilage zone interdigitates with the trabecular bone (wavy arrow). There are also areas of degenerated bone and bone marrow (\*). (H&E, X200)

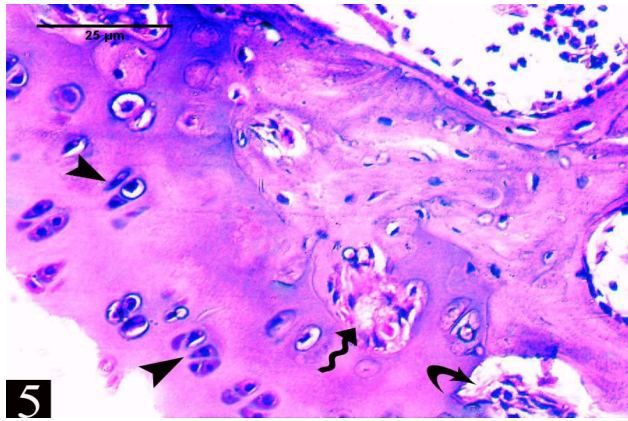


**Fig. 5:** A photomicrograph of the articular cartilage of the rat knee joint from group II showing chondrocyte aggregation (arrow head) and degenerative changes in the bone matrix (wavy arrow). Bone marrow spaces (curved arrow) are filled with inflammatory cells. (H&E, X400)

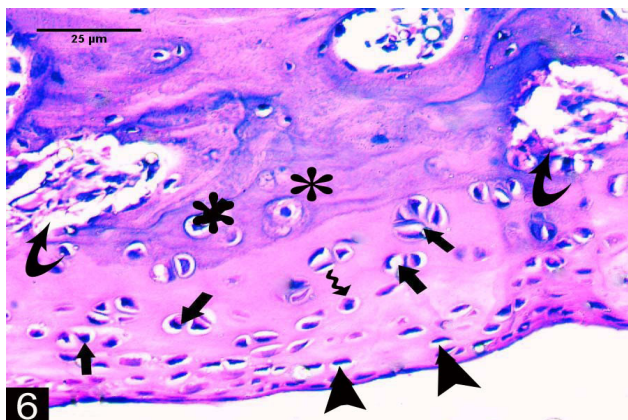


**Fig. 6:** A photomicrograph of the articular cartilage of the rat knee joint from group II showing many chondrocytes with flat nuclei in the superficial zone (arrow head), rounded chondrocytes of intermediate zone (wavy arrow), aggregated chondrocytes (arrow) in the deep zone and the tide mark. Notice, Bone marrow spaces containing inflammatory cells and are in contact with the articular cartilage (curved arrow). The calcified cartilage interdigitates with bone with many cement lines (\*). (H&E, X400)

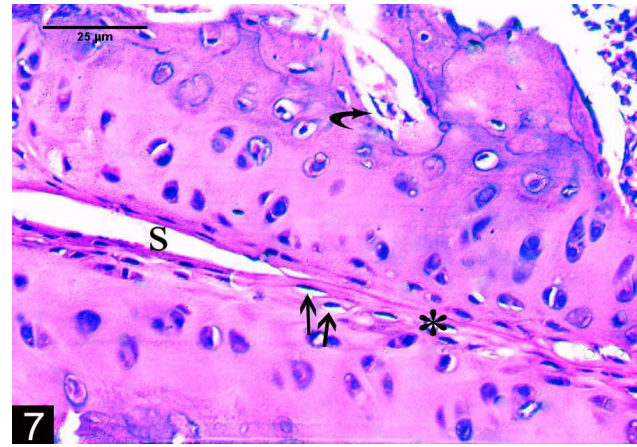


**Fig. 7:** A photomicrograph of the articular cartilage of the rat knee joint from group II showing narrowing of the joint space (S) with focal adhesion of the two articular cartilages (\*). Notice degenerated superficial cells (arrow) and invasion of bone marrow cells into the articular cartilage (curved arrow). (H&E, X400)

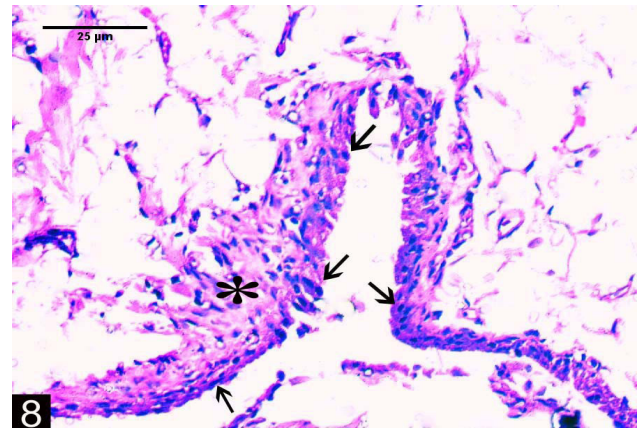


**Fig. 8:** A photomicrograph of the synovial membrane of the rat knee joint from group II showing absence of the intimal folds and several cell rows of synoviocytes (arrow). The subintimal zone shows inflammatory cellular infiltration (\*). (H&E, X400)

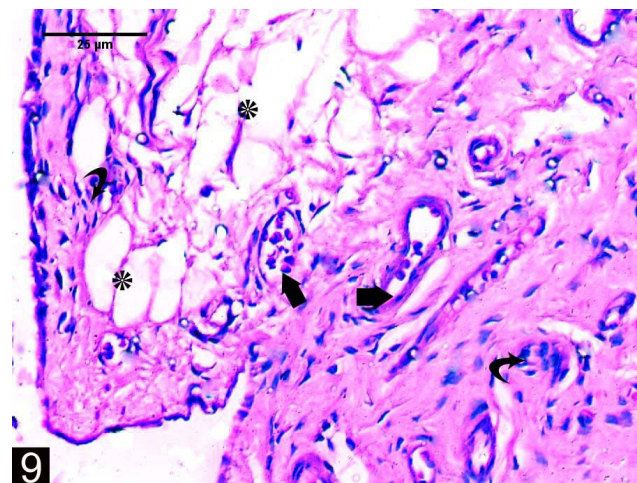


**Fig. 9:** A photomicrograph of the synovial membrane of the rat knee joint from group II showing loosely arranged collagen fibers in the superficial subintimal zone (\*) and closely packed fibers with many blood vessels (arrow) and inflammatory cells (curved arrow) in the deep subintimal zone. (H&E, X400)

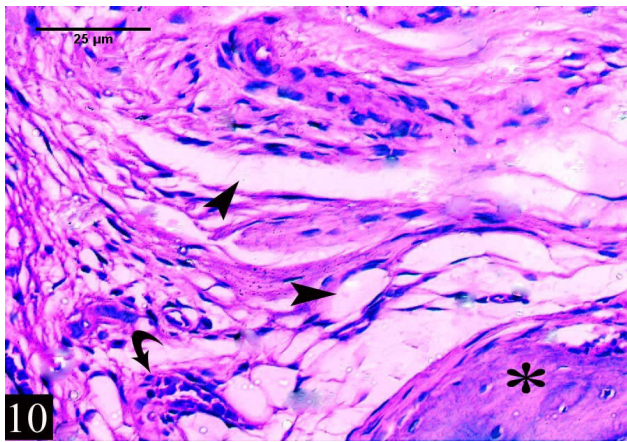


**Fig. 10:** A photomicrograph of the synovial membrane of the rat knee joint from group II showing mononuclear cellular infiltration (curved arrow). Collagen fibers are separated by spaces of edema (arrow head). Notice proliferation of the synovium over the articular cartilage (\*). (H&E, X400)

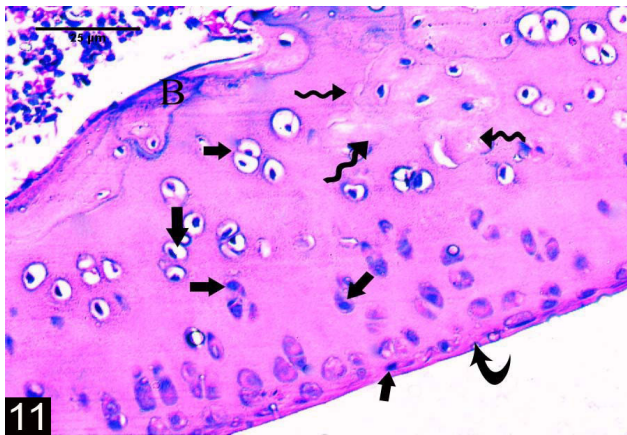


**Fig. 11:** A photomicrograph of the articular cartilage of the rat right knee joint from subgroup III-a (BM-MS treated group) showing smooth surface with apparent increase in its thickness (curved arrow) and some degenerated chondrocytes (arrow). The calcified cartilage zone interdigitates with the trabecular bone (wavy arrow). Notice apparent thin area of subchondral bone (B). (H&E, X400)

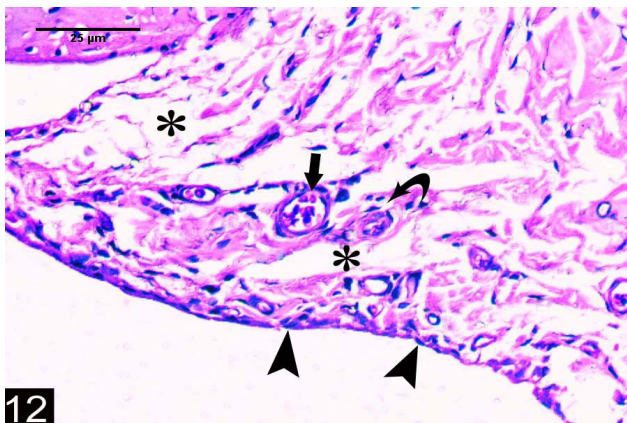


**Fig. 12:** A photomicrograph of the synovial membrane of the rat right knee joint from subgroup III-a (BM-MS treated group) showing two cell layers of the intima (arrow head) with a few congested blood vessels (arrow). Notice separated subintimal collagen fibers by spaces of edema (\*) and mononuclear cellular infiltration (curved arrow) of the subintima. (H&E, X400)

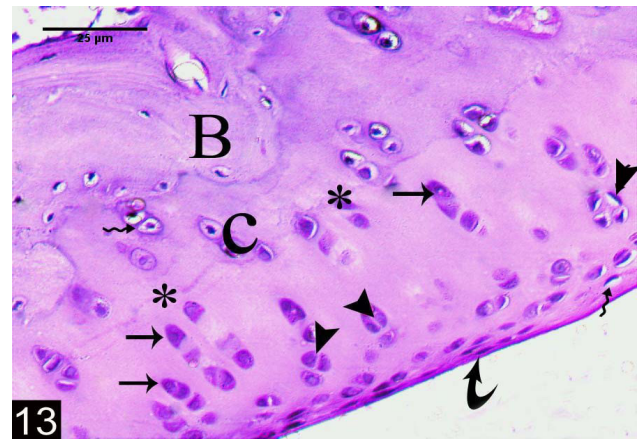


**Fig. 13:** A photomicrograph of the articular cartilage of the rat left knee joint from subgroup III-b (MS-C treated group) showing smooth surface with apparent normal thickness (curved arrow), normal zonal arrangement (arrow head) and columnar orientation (arrow) of the chondrocytes with intact tide mark (\*) separating the calcified zone (C) from other zones. The calcified cartilage zone contains chondrocytes with apoptotic nuclei (wavy arrow). Notice apparent thick area of the subchondral bone (B). (H&E, X400)

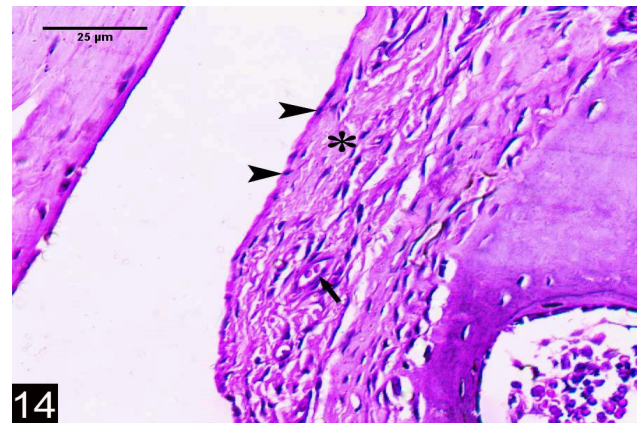


**Fig. 14:** A photomicrograph of the synovial membrane of the rat left knee joint from subgroup III-b (MS-C treated group) showing single cell layer of the intima (arrow head) and the subintimal layer of connective tissue containing fibroblasts, collagen fibers (\*) and blood vessels (arrow). (H&E, X400)

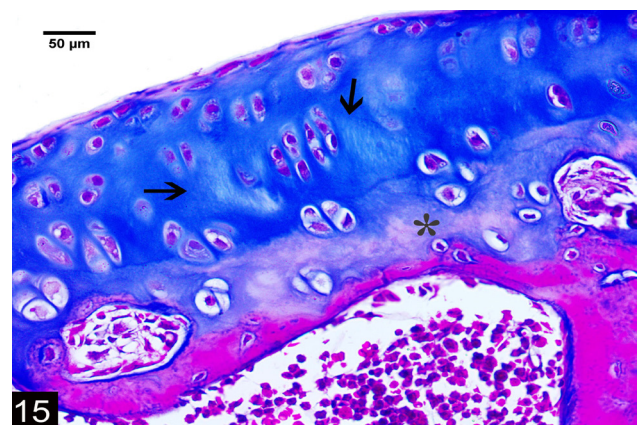


**Fig. 15:** A photomicrograph of the articular cartilage of the rat knee joint from group I showing normal collagen fibers distribution in the uncalcified (arrow) and calcified (\*) zones. (Masson's trichrome, X400)

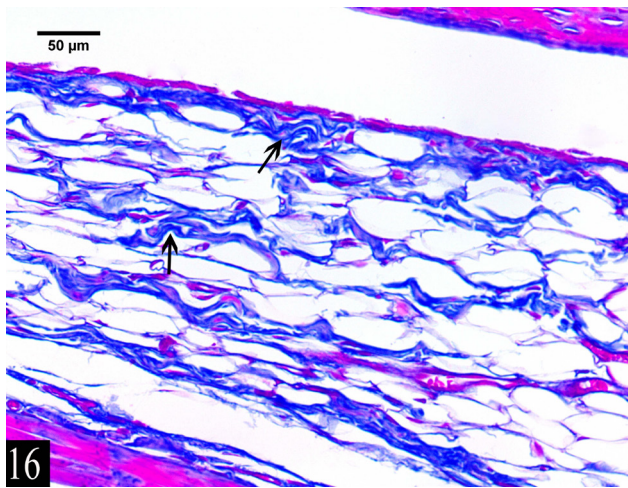


**Fig. 16:** A photomicrograph of the synovial membrane of the rat knee joint from group I showing a few collagen fibers (arrow) in the subintima. (Masson's trichrome, X400)

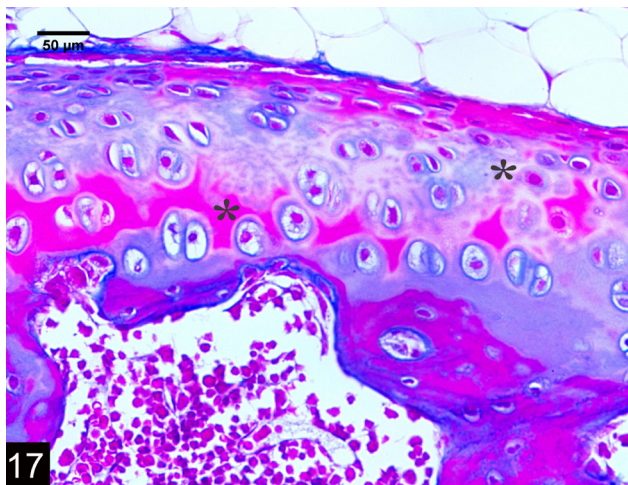


**Fig. 17:** A photomicrograph of the articular cartilage of the rat knee joint from group II showing marked apparent decrease in the collagen fibers of all zones (\*).(Masson's trichrome, X400)

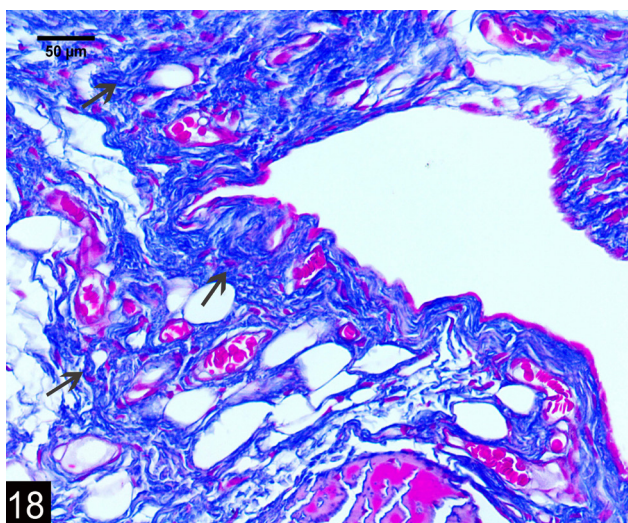


**Fig. 18:** A photomicrograph of the synovial membrane of the rat knee joint from group II showing abundant subintimal collagen fibers deposition (arrow). (Masson's trichrome, X400)

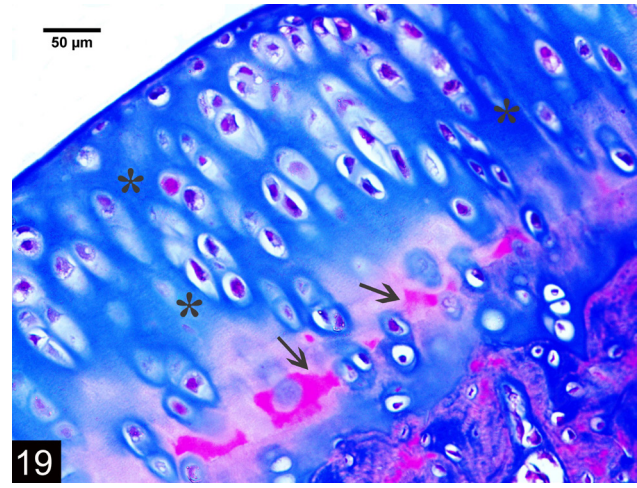


**Fig. 19:** A photomicrograph of the articular cartilage of the rat right knee joint from subgroup III-a (BM-MS treated group) showing apparently increased collagen fibers of all zones (\*). Notice a few areas with decreased collagen (arrow). (Masson's trichrome, X400)

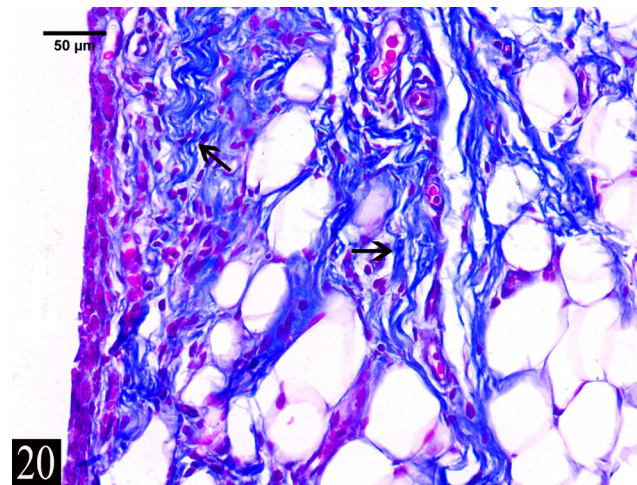


**Fig. 20:** A photomicrograph of the synovial membrane of the rat right knee joint from subgroup III-a (BM-MS treated group) showing a moderate amount of collagen fibers in the subintima (\*). (Masson's trichrome, X400)

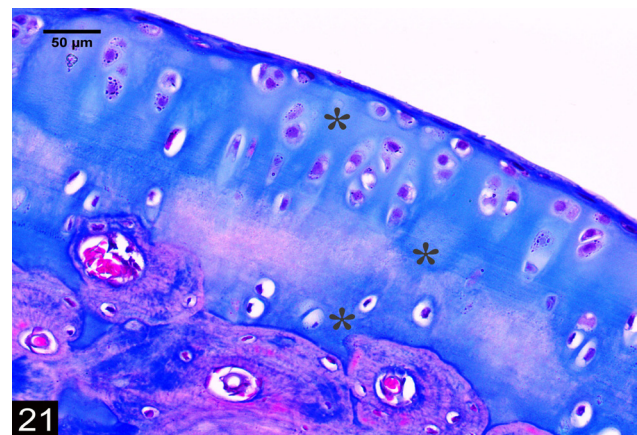


**Fig. 21:** A photomicrograph of the articular cartilage of the rat left knee joint from subgroup III-b (MS-C treated group) showing apparently increased collagen fibers of all zones (\*). (Masson's trichrome, X400)

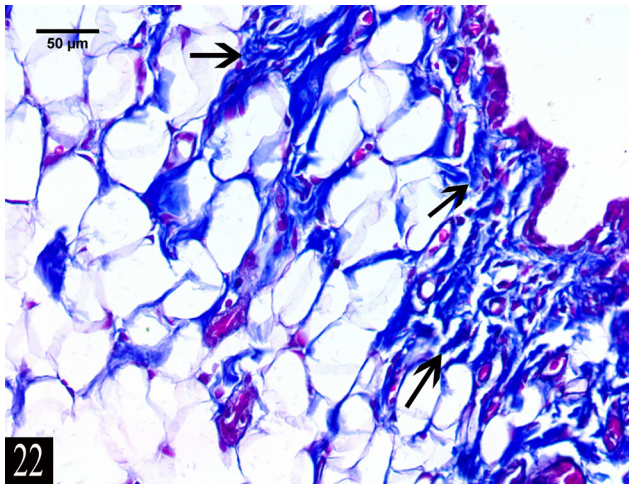


**Fig. 22:** A photomicrograph of the synovial membrane of the rat left knee joint from subgroup III-b (MS-C treated group) showing a moderate amount of collagen fibers in the subintima (\*).(Masson's trichrome, X400)

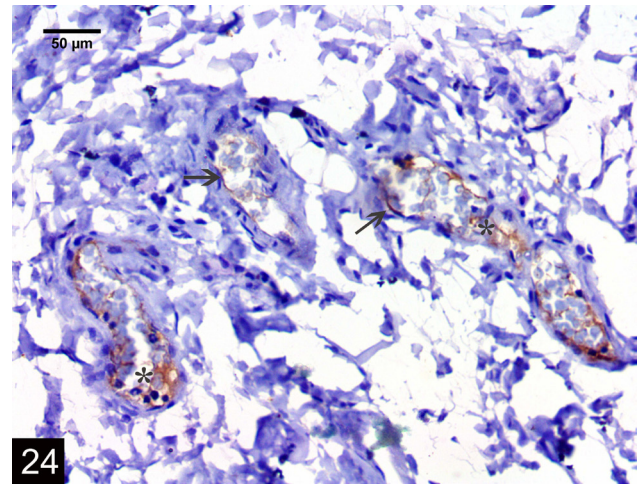


**Fig. 24:** A photomicrograph of the synovial membrane of the rat knee joint from group II showing a strong positive UPA immunoreactivity in the wall of the blood vessels (arrow) and in the intravascular cells (\*). (UPA immunostaining, X400)

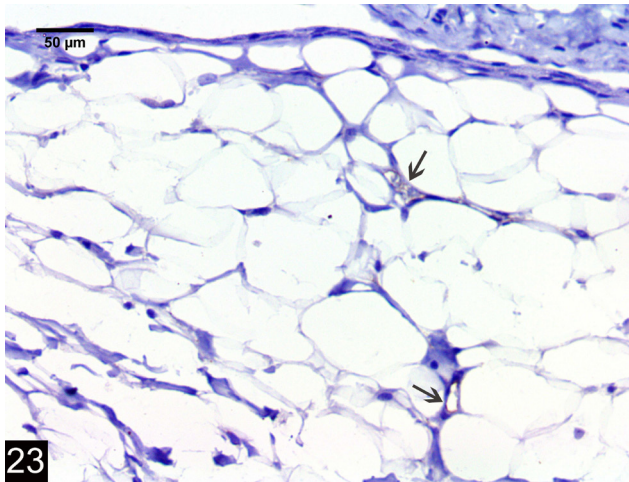


**Fig. 23:** A photomicrograph of the synovial membrane of the rat knee joint from group I showing a faint positive immunoreactivity for UPA in the wall of the blood vessels (arrow). (UPA immunostaining, X400)

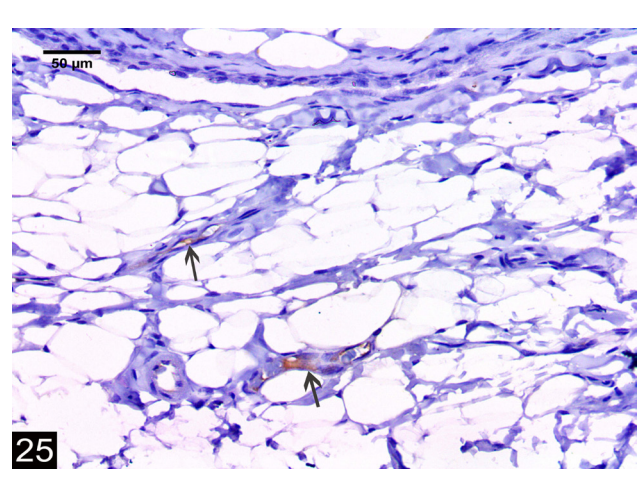


**Fig. 25:** A photomicrograph of the synovial membrane of the rat right knee joint from subgroup III-a (BM-MS treated group) showing a weak positive UPA immunoreactivity in the blood vessels (arrow). (UPA immunostaining, X400)

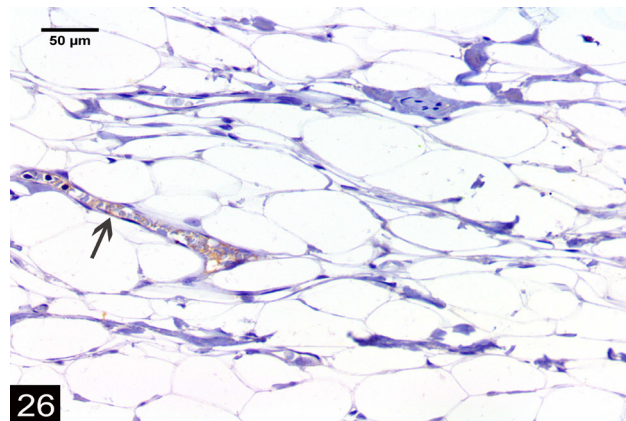


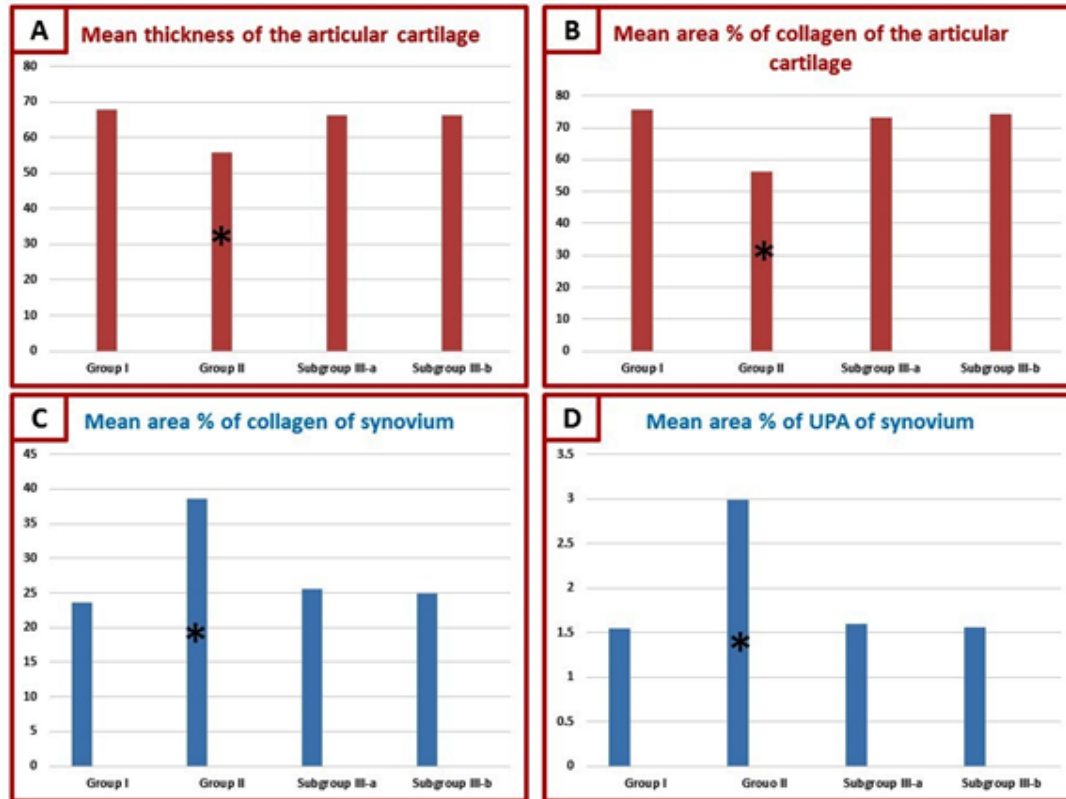
**Fig. 26:** A photomicrograph of the synovial membrane of the rat left knee joint from subgroup III-b (MS-C treated group) showing a weak positive UPA immunoreactivity in the blood vessels (arrow). (UPA immunostaining, X400)

**Table 1:** Morphometric analysis of the knee joint specimens of all groups (Mean ± SD)

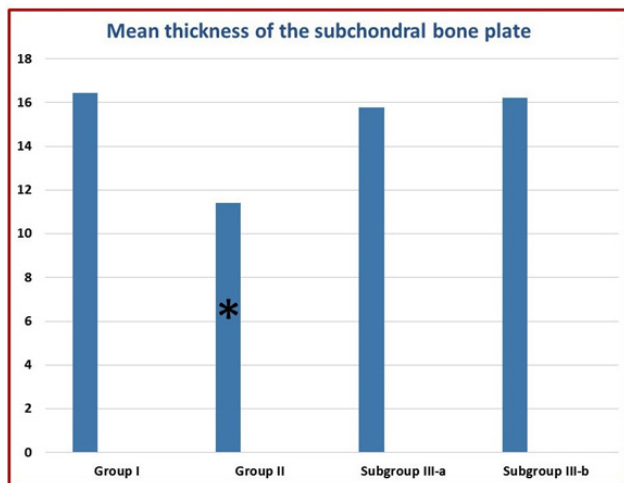
Parameters	Group 1 (control group)	Group II (SS-associated arthritis group)	Subgroup III-a (BM-MS treated group)	Subgroup III-b (MS-C treated group)
Mean articular cartilage thickness (µm)	67.80± 2.91	55.83±3.50*	66.24±2.92**	66.30±3.16**
Mean subchondral bone plate thickness (µm)	16.431±0.878	11.42±1.42*	15.779±0.581**	16.207±0.903**
Mean area % of collagen of articular cartilage	75.59±2.73	56.29±5.23*	73.37±3.21**	74.30±3.17**
Mean area % of collagen of synovium	23.63±1.92	38.61±6.23*	25.56±2.73**	24.92±2.59**
Mean area % of UPA of synovium	1.542±0.293	2.985±0.570*	1.599±0.240**	1.553±0.219**

\*P < 0.05 is significant versus group I.

\*\*P < 0.05 is non-significant versus group I.



**Histogram 1:** Morphometrical and statistical analysis of [A] Mean articular cartilage thickness. [B] Mean area % of collagen of the articular cartilage. [C] Mean area % of collagen of synovium [D] Mean area % of UPA immuno-expression of synovium. \* Indicates significance vs control.



**Histogram 2:** Morphometric and statistical analysis of the mean thickness of the subchondral bone plate in all study groups. \* Indicates significance vs control.

**DISCUSSION**

Systemic sclerosis is a chronic autoimmune connective tissue disorder. Arthritis is considered a frequent manifestation for SS that plays a role in the morbidity of this disorder due to pain and disability<sup>[9,33,34]</sup>. Extensive studies on application of BM-MS and MS-C are currently underway due to their effects on tissue regeneration<sup>[14,20]</sup>. So, this experimental study was designed to explore novel pathways involved in systemic sclerosis associated arthritis and to compare the therapeutic effects of the mesenchymal stem cells and their conditioned medium on knee joint arthritis associated with bleomycin induced model of systemic sclerosis in adult male albino rats.

The histological results of this study revealed knee joint arthritis associated with bleomycin induced model of systemic sclerosis in adult male albino rats. Also, the study revealed therapeutic effects of the intra articular injection of BM-MS and MS-C on the joint structure.

However, MS-C induced marked improvement of the joint structure which was greater than that of the mesenchymal stem cells. So, MS-C injection fastened the healing process of the articular cartilage, subchondral bone and synovium reaching more or less to the control ones. Moreover, the immunohistochemical findings of our study suggested the possible role of UPA pathway in the pathogenesis of systemic sclerosis associated arthritis.

The present study showed that systemic sclerosis associated arthritis of the knee joint was manifested histologically by degenerated articular cartilage and subchondral bone in addition to synovitis. The articular cartilage showed surface irregularity, erosion, clefts, complete disorganization, matrix loss, disturbed columnar orientation in addition to degenerated subchondral bone. Moreover, there was inflammation of the synovium which was manifested by vascular congestion, edema and inflammatory cellular infiltration in addition to synoviocyte hyperplasia with subintimal fibrosis and proliferation of the synovium over the articular cartilage. Moreover, there was an increased immuno-expression of UPA in the inflamed synovium. The morphometrical and statistical evaluation confirmed the light microscopic findings. It revealed significant decrease in articular cartilage and subchondral bone plate thickness, decreased collagen content of the matrix of the articular cartilage and marked subintimal collagen deposition. Our results coincided with previous studies which reported that hyperplasia of the synovial lining and inflammatory infiltrate in the synovium with erosion of the articular cartilage and subchondral bone are main histological manifestations for arthritis<sup>[35]</sup>. Systemic sclerosis is associated with changes as inflammatory, fibrotic and degenerative processes. So, it could induce inflammatory arthritis manifested by articular and bone erosion, joint space narrowing, joint effusion and synovial thickening<sup>[9]</sup>.

In this study, the observed inflammation and fibrosis may be through the activation of transforming growth factor-Beta (TGF- $\beta$ ), fibroblasts and P53 resulting in fibrosis and also apoptosis. Also, the inflammation could be mediated by increasing tumor necrosis factor alpha (TNF- $\alpha$ ), IL-1 and 6 initiating fibrosis<sup>[1]</sup>.

Normally, the turnover and/or accumulation of the extracellular matrix proteins are regulated by an interaction of matrix metalloproteinases (MMPs) and inhibitors of metalloproteinases in tissues. In SS, there is dysregulation of these proteolytic and inhibitory proteins leading to tissue fibrosis<sup>[36]</sup>.

Bleomycin could induce oxidative damage to nucleic acids. So, oxidative stress may play a role in triggering autoimmunity by promoting the differentiation of B-cell to increase antibody production or autoantibodies resulting in all pathological manifestations of SS namely, inflammatory and fibrotic processes. In turn, these pathological processes could induce reactive oxygen species overproduction to maintain a vicious cycle. ROS also cause fibroblasts

activation and trigger the synthesis of pro-inflammatory cytokines from immune cells such as IL-1 $\beta$ . In addition, ROS could modulate TGF- $\beta$  which is a potent pro-fibrotic cytokine in the fibrotic process. TGF- $\beta$  could activate fibroblasts to differentiate into myofibroblasts leading to increased collagen production. ROS also could activate latent MMPs pro-enzymes and mediate the IL-1 $\beta$ -dependent MMP-9 induction. ROS may be responsible for the imbalance of MMPs and their inhibitors in SS. All these data prove the role of oxidative stress in SS pathogenesis leading to inflammation and fibrosis<sup>[37,38]</sup>.

So, damage and destruction of the articular cartilage of the present study may be caused by inflammation. Subsequently, the proinflammatory cytokines (IL-1 $\beta$  & IL-6) and TNF- $\alpha$  are upregulated in joint tissues and synovial fluid leading to pathogenesis of arthritis. Moreover, IL-1 $\beta$  and TNF- $\alpha$  suppress the expression of extracellular matrix (ECM) components of the cartilage<sup>[15]</sup>. Also, these mediators could suppress the antioxidant enzymes production that scavenge ROS. They could stimulate nuclear factor kappa-B signaling that trigger articular cartilage degeneration by upregulation of MMPs<sup>[14]</sup>.

Also, the destruction of the subchondral bone with a statistically significant decrease in its thickness in this study was attributed to the increased osteoclast number in arthritis by increased cytokine synthesis<sup>[39]</sup>. Systemic sclerosis is associated by bone erosion and thinning of the subchondral bone plate<sup>[40]</sup>. In systemic sclerosis, there is increased osteoclasts activity and osteoclastogenesis due to vasculopathy and hypoxia leading to bone erosion<sup>[41]</sup>.

In addition, the immunohistochemical findings of this study suggested the possible role of UPA pathway in the pathogenesis of systemic sclerosis associated arthritis. Our results revealed increased UPA expression in the inflamed synovium which was statistically significant compared to control group. Urokinase plasminogen activator (UPA) is a proinflammatory mediator that has a role in cartilage and bone destruction in arthritis. Its expression is elevated in osteoarthritis<sup>[42,43]</sup>. It is expressed in the vascular endothelium, intravascular macrophage and neutrophils of synovial blood vessels<sup>[44]</sup>. Moreover, systemic sclerosis is associated with elevated plasma level of UPA and UPA receptor<sup>[45]</sup>. In inflamed joint, UPA production is elevated. It is released into the inflamed joint cavity to convert plasminogen into plasmin. Plasmin is an enzyme which is able to degrade not only fibrin but also the extracellular matrix of the hyaline cartilage. Additionally, UPA binds to UPA receptors present on the cell surface promoting proteolysis. UPA and plasmin can also activate MMPs leading to joint cartilage destruction<sup>[43,46,47]</sup>.

The present study demonstrated the therapeutic effect of BM-MS on the articular cartilage, subchondral bone and synovial membrane. This may be attributed to their great potential in the regeneration of chondrocytes and differentiation into cartilage in addition to their anti-inflammatory and immunoregulatory effects<sup>[15]</sup>.

In inflammation, BM-MS response by homing into the inflamed tissue, modulating immune and inflammatory responses and helping in repairing of the damaged area. They suppress of T-lymphocyte, antigen presenting cell and the pro-inflammatory cytokines and chemokines. These effects may be mediated directly by cell to cell contact or by the release of soluble factors or cytokines with subsequent resolution of the inflammation. BM-MS could initiate cartilage repair by chondrogenic proliferation and the secretion of ECM proteases and growth factors. They may be differentiated into chondrocytes or promoting the proliferation of the remaining chondroprogenitors by secretion of trophic factors enhancing cartilage regeneration and reducing synovial inflammation<sup>[14,48]</sup>. Moreover, BM-MS could reduce subchondral bone erosion by inhibiting osteoclast activity and differentiation<sup>[49,50]</sup>.

BM-MS can perform their effects by release of secretory factors in their conditioned medium as extracellular vesicles. Exosomes (a subtype of extracellular vesicles) transmit numerous proteins as growth factors and cytokines through these vesicles to regenerate the damaged cells and modulate the immune response<sup>[48]</sup>. This explanation was in accordance with our results that demonstrated marked improvement of the joint structure after intra-articular MS-C injection which was greater than that of the BM-MS.

Exosomes of MS-C are heterogeneous membranous vesicles containing various bioactive molecules such as proteins, lipids, RNAs and DNA. These molecules are important in intercellular communication to regulate wide range pathways<sup>[51]</sup>. The secretomes of MS-C could regulate numerous cell activities as extracellular matrix synthesis, cell proliferation, differentiation and migration. Their bioactive molecules may activate resting stem cells or restoring activity of the injured ones. They increase anabolic markers (as collagen type II & aggrecan) of chondrocytes, inhibit catabolic and inflammatory markers to reduce articular cartilage damage. They act also by decreasing inflammatory mediators (as TNF- alpha, IL-6) and MMPs activity and increasing the anti-inflammatory cytokine IL-10. So, they regulate immune response, induce cartilage regeneration, diminish apoptosis and ameliorate synovial inflammation<sup>[25,52]</sup>. Moreover, secretomes of MS-C possess antioxidant role in injured tissues including the joints<sup>[17,53]</sup>. They are also able to promote osteoblasts and inhibit osteoclasts regulating bone remodeling<sup>[54,55]</sup>.

The therapeutic effects of MS-C in osteoarthritis are also attributed to microRNA (miRNA), which is an important component of the exosomes (a subtype of extracellular vesicles)<sup>[56,57]</sup>. Micro RNA could alleviate the damage of the articular cartilage, subchondral bone and synovial membrane<sup>[58,59]</sup>. Secretomes of MS-C could downregulate IL-1 $\beta$  reducing the inflammatory process and apoptosis<sup>[60,61]</sup>. Moreover, the extracellular vesicles of the conditioned medium of bone marrow stem cells have a stronger effect on promoting chondrocyte proliferation compared with the others of different anatomic location<sup>[62,63]</sup>. They also could attenuate subchondral bone destruction by

osteoclastogenesis inhibition<sup>[64]</sup>. Extracellular vesicles also could activate Plasminogen activator inhibitor 1 (PAI-1) in endothelial cells of inflamed synovium suppressing UPA/UPA receptor pathway and inhibiting its proteolytic effect on the extracellular matrix. So, PAI-1 help in reducing joint inflammation and fibrosis<sup>[65,66]</sup>. This coincided with our immunohistochemical findings of reduced UPA expression of the synovium.

## CONCLUSION

---

This study revealed systemic sclerosis associated arthritis in the knee joint of adult male albino rats. The study also suggests the possible participation of UPA/UPA receptor pathway in the development of arthritis. Moreover, both BM-MS and MS-C induced articular cartilage and subchondral bone regeneration and decreased synovial inflammation. However, our results showed that MS-C possesses better therapeutic effects than BM-MS. So, MS-C fastened the healing process and can be considered as a potential therapeutic tool for SS-associated arthritis of the knee joint.

## ACKNOWLEDGMENT

---

Many thanks to Dr. Amany Mohammed Elshawarby, Professor of Histology and Cell Biology, Faculty of Medicine, Ain-Shams University for her effort, help and experience in tissue culture.

## CONFLICT OF INTERESTS

---

There are no conflicts of interest.

## REFERENCES

---

1. Yamamoto Y, Okano T, Yamada H, Akashi K, Sendo S, Ueda Y, Morinobu A, Saegusa J: Soluble guanylate cyclase stimulator reduced the gastrointestinal fibrosis in bleomycin-induced mouse model of systemic sclerosis. *Arthritis Res Ther* 23, 133 (2021). <https://doi.org/10.1186/s13075-021-02513-y>
2. Romano E, Rosa I, Fioretto BS, Matucci-Cerinic M, Manetti M: New Insights into Profibrotic Myofibroblast Formation in Systemic Sclerosis: When the Vascular Wall Becomes the Enemy. *Life (Basel)*. 2021 Jun 24;11(7):610. doi: 10.3390/life11070610. PMID: 34202703; PMCID: PMC8307837.
3. Asano Y: Systemic sclerosis. *The Journal of Dermatology* (2018) 45:128-138. <https://doi.org/10.1111/1346-8138.14153>
4. Abignano G, Hermes H, Piera-Velazquez S, Addya S, Del Galdo F, Jimenez SA: Global gene expression analysis of systemic sclerosis myofibroblasts demonstrates a marked increase in the expression of multiple NBPF genes. *Sci Rep*. 2021 Oct 14;11(1):20435. doi: 10.1038/s41598-021-99292-y. PMID: 34650102; PMCID: PMC8516909.

5. Shima, Y: Cytokines involved in the pathogenesis of SSc and problems in the development of anti-cytokine therapy. *Cells*. 2021 May 4;10(5):1104. doi: 10.3390/cells10051104. PMID: 34064515; PMCID: PMC8147957.
6. Rosa I, Romano E, Fioretto BS, Manetti M: The contribution of mesenchymal transitions to the pathogenesis of systemic sclerosis. *Eur J Rheumatol*. 2020 Oct;7(Suppl 3):S157-S164. doi: 10.5152/eurjrheum.2019.19081. Epub 2019 Dec 19. PMID: 31922472; PMCID: PMC7647682.
7. Waszczykowski M, Dzionkowska-Bartkowiak B, Podgórski M, Fabiś J, Waszczykowska A: Role and effectiveness of complex and supervised rehabilitation on overall and hand function in systemic sclerosis patients—one-year follow-up study. *Sci Rep*. 2021 Jul 26;11(1):15174. doi: 10.1038/s41598-021-94549-y. PMID: 34312449; PMCID: PMC8313718.
8. Azarbani N, Javadzadeh A, Mohseni I, Jalali A, Andalib E, Poormoghim H: Association of musculoskeletal and radiological features with clinical and serological findings in systemic sclerosis: A single-centre registry study. *Mediterr J Rheumatol*. 2020 Sep 30;31(3):341-349. doi: 10.31138/mjr.31.3.341. PMID: 33163868; PMCID: PMC7641026.
9. Blank RB, Nwawka OK, Yusov AA, Gordon Jk: Inflammatory arthritis in systemic sclerosis: What to do? *J Scleroderma Relat Disord*. 2019 Feb;4(1):3-16. doi: 10.1177/2397198318779532. Epub 2018 Jun 19. PMID: 35382152; PMCID: PMC8922577.
10. Varju C, Pentek M, Lorand V, Nagy G, Minier T, Czirjak L: Musculoskeletal involvement in systemic sclerosis: an unexplored aspect of the disease. *JSRD* (2017) 2(1): 19-32. DOI:10.5301/jsrd.5000228
11. MOLINA-RIOS Sebastian, ORDONEZ C Eliana, QUINTANA-LOPEZ Gerardo: Osteoarticular manifestations of systemic sclerosis: a systematic review of the literature. *Rev Colomb Reumatol*. (2020) 27(S1):85–110. <https://doi.org/10.1016/j.rcreu.2019.11.006>
12. Tang J, Zhou X, Wu X, Lin S, Ming B, Zhong J, Wang B and Dong L: Gut Microbiota Aberration in Patients of Systemic Sclerosis and Bleomycin-Induced Mice Model. *Front Cell Infect Microbiol*. 2021 May 28;11:647201. doi: 10.3389/fcimb.2021.647201. PMID: 34123867; PMCID: PMC8193929.
13. Al-Dhamin Z, Liu LD, Li DD, Zhang SY, Dong SM, Nan YM: Therapeutic efficiency of bone marrow-derived mesenchymal stem cells for liver fibrosis: A systematic review of *in vivo* studies. *World J Gastroenterol*. 2020 Dec 21;26(47):7444-7469. doi: 10.3748/wjg.v26.i47.7444. PMID: 33384547; PMCID: PMC7754546.
14. Nurul AA, Azlan M, Ahmad Mohd Zain MR, Sebastian AA, Fan YZ, Fauzi MB: Mesenchymal stem cells: current concepts in the management of inflammation in osteoarthritis. *Biomedicines*. 2021 Jul 7;9(7):785. doi: 10.3390/biomedicines9070785. PMID: 34356849; PMCID: PMC8301311.
15. Zhu C, Wu W, Qu X: Mesenchymal stem cells in osteoarthritis therapy: a review. *Am J Transl Res*. 2021 Feb 15;13(2):448-461. PMID: 33594303; PMCID: PMC7868850.
16. Chen W, Sun Y, Gu X, Hao Y, Liu X, Lin J, Chen J, Chen S: Conditioned medium of mesenchymal stem cells delays osteoarthritis progression in a rat model by protecting subchondral bone, maintaining matrix homeostasis and enhancing autophagy. *J Tissue Eng Regen Med*. 2019 Sep;13(9):1618-1628. doi: 10.1002/term.2916. Epub 2019 Jul 2. PMID: 31210406.
17. Kim KH, Jo JH, Cho HJ, Park TS, Kim TM: Therapeutic potential of stem cell-derived extracellular vesicles in osteoarthritis: preclinical study findings. *Lab Anim Res*. 2020 Apr 15;36:10. doi: 10.1186/s42826-020-00043-3. PMID: 32322556; PMCID: PMC7160998.
18. Takeuchi R, Katagiri W, Endo S, Kobayashi T: Exosomes from conditioned media of bone marrow derived mesenchymal stem cells promote bone regeneration by enhancing angiogenesis. *PLoS One*. 2019 Nov 21;14(11):e0225472. doi: 10.1371/journal.pone.0225472. PMID: 31751396; PMCID: PMC6872157.
19. Foo JB, Looi QH, How CW, Lee SH, Al-Masawa ME, Chong PP, Law JX: Mesenchymal stem cell-derived exosomes and microRNAs in cartilage regeneration: biogenesis, efficacy, miRNA enrichment and delivery. *Pharmaceuticals* (2021) 14(11):1093. <http://dx.doi.org/10.3390/ph14111093>
20. Kusuma HSW, Widowati W, Gunanegara RF, Juliandi B, Lister NE, Arumwardana S, Yusepany DT, Artie DS, Nataya ED, Gunawan KY, Sholihah IA, Girsang E, Ginting CN, Bachtiar I, Murti H: Effect of conditioned medium from IGF1-induced human wharton's jelly mesenchymal stem cells (IGF1-hWJMSCs-CM) on osteoarthritis. *Avicenna J Med Biotechnol*. 2020 Jul-Sep;12(3):172-178. PMID: 32695280; PMCID: PMC7368112.
21. Nabavizadeh SS, Talaei-Khozani T, Zarei M, Zare S, Hosseinabadi OK, Tanideh N, Daneshi S: Attenuation of osteoarthritis progression through intra-articular injection of a combination of synovial membrane-derived MSCs (SMMSCs), platelet-rich plasma (PRP) and conditioned medium (secretome). *J Orthop Surg Res*. 2022 Feb 17;17(1):102. doi: 10.1186/s13018-021-02851-2. PMID: 35177103; PMCID: PMC8851803.

22. Taghiyar L , Jahangir S , Ravari MK , Shamekhi MA, Eslaminejad MB: Cartilage repair by mesenchymal stem cell-derived exosomes: preclinical and clinical trial update and perspectives. *Adv Exp Med Biol.* 2021;1326:73-93. doi: 10.1007/5584\_2021\_625. PMID: 33629260.
23. Huang S, Xu L, Sun Y, Wu T, Wang K, Li G: An improved protocol for isolation and culture of mesenchymal stem cells from mouse bone marrow. *J Orthop Translat.* 2014 Aug 27;3(1):26-33. doi: 10.1016/j.jot.2014.07.005. PMID: 30035037; PMCID: PMC5982388.
24. Abouelnaga H, El-Khateeb D, Moemen Y, El-Fert A, Elgazzar M, Khalil A. Characterization of mesenchymal stem cells isolated from Wharton's jelly of the human umbilical cord. *Egypt Liver Journal* 12, 2 (2022). <https://doi.org/10.1186/s43066-021-00165-w>
25. Chen YC, Chang YW, Tan KP, Shen YS, Wang YH, Chang CH: Can mesenchymal stem cells and their conditioned medium assist inflammatory chondrocytes recovery? *PLoS One.* 2018 Nov 21;13(11):e0205563. doi: 10.1371/journal.pone.0205563. PMID: 30462647; PMCID: PMC6248915.
26. Juniantito V, Izawa T, Yuasa T, Ichikawa C, Yano R, Kuwamura M, Yamate J: Immunophenotypical characterization of macrophages in rat bleomycin-induced scleroderma. *Vet Pathol.* 2013 Jan;50(1):76-85. doi: 10.1177/0300985812450718. Epub 2012 Jun 13. PMID: 22700848.
27. Pitcher T, Sousa-Valente J, Malcangio M: The monoiodoacetate model of osteoarthritis pain in the mouse. *J Vis Exp.* 2016 May 16;(111):53746. doi: 10.3791/53746. PMID: 27214709; PMCID: PMC4942175.
28. Gaertner DJ, Hallman TM, Hankenson FC, Batcherder MA (2008): *Anesthesia and Analgesia in Rodents. Anesthesia and analgesia in laboratory animals. 2nd edition.* Academic Press, San Diego, CA. Boston. P: 239-240.
29. Suvarna S, Layton C, Bancroft J (2013): *Bancroft's theory and practice of histological techniques.* 7th edition, Elsevier. Chapter 16, P: 317-352.
30. Bancroft J, Christophe L, kim S (2013): *Bancroft's theory and practice of histological techniques.* 7th edition, Churchill Livingstone. P:179-202.
31. Ramos-Vara JA, Kiupel M, Baszler T, Bliven L, Brodersen B, Chelack B, Czub S, Del Piero F, Dial S, Ehrhart EJ, Graham T, Manning L, Paulsen D, Valli VE, West K: American Association of Veterinary Laboratory Diagnosticians Subcommittee on Standardization of Immunohistochemistry. Suggested guidelines for immunohistochemical techniques in veterinary diagnostic laboratories. *J Vet Diagn Invest.* 2008 Jul;20(4):393-413. doi: 10.1177/104063870802000401. PMID: 18599844.
32. Dawson-Saunders B and Trapp R (2001). *Basic and clinical biostatistics.* 3rd ed., Lang Medical Book, McGraw Hill Medical Publishing Division. 161-218.
33. Schmeiser T , Pons-Kühnemann J, Özden F, Müller-Ladner U, Dinser R: Arthritis in patients with systemic sclerosis. *Eur J Intern Med.* 2012 Jan;23(1):e25-9. doi: 10.1016/j.ejim.2011.09.010. Epub 2011 Oct 20. PMID: 22153544.
34. Sobolewski P, Maślińska M, Wieczorek M, Łagun Z, Malewska A, Roszkiewicz M, Nitskovich R, Szymańska E, Walecka I: Systemic sclerosis–multidisciplinary disease: clinical features and treatment. *Reumatologia.* 2019;57(4):221-233. doi: 10.5114/reum.2019.87619. Epub 2019 Aug 31. PMID: 31548749; PMCID: PMC6753596.
35. Knoerzer DB, Donovan MG, Schwartz BD, Mengle-Gaw LJ: Clinical and histological assessment of collagen-induced arthritis progression in the diabetes-resistant BB/Wor rat. *Toxicol Pathol.* 1997 Jan-Feb;25(1):13-9. doi: 10.1177/019262339702500103. PMID: 9061845.
36. Leong E, Bezuhly M and Marshall JS: Distinct metalloproteinase expression and functions in systemic sclerosis and fibrosis: what we know and the potential for intervention. *Front Physiol.* 2021 Aug 27;12:727451. doi: 10.3389/fphys.2021.727451. PMID: 34512395; PMCID: PMC8432940.
37. Doridot L, Jelieli M, Chene C, Batteux F: Implication of oxidative stress in the pathogenesis of systemic sclerosis via inflammation, autoimmunity and fibrosis. *Redox Biol* (2019) 25: 101122. <https://doi.org/10.1016/j.redox.2019.101122>
38. Sierra-Sepúlveda A, Esquinca-González A, Benavides-Suárez SA, Sordo-Lima DE, Caballero-Islas AE, Cabral-Castañeda AR, Rodríguez-Reyna TS: Systemic sclerosis pathogenesis and emerging therapies beyond the fibroblast. *Biomed Res Int.* 2019 Jan 23;2019:4569826. doi: 10.1155/2019/4569826. PMID: 30809542; PMCID: PMC6364098.
39. Zhu X, Chan YT, Yung PSH, Tuan RS and Jiang Y: Subchondral Bone Remodeling: A Therapeutic Target for Osteoarthritis. *Front Cell Dev Biol.* 2021 Jan 21;8:607764. doi: 10.3389/fcell.2020.607764. PMID: 33553146; PMCID: PMC7859330.
40. Ramonda R, Del Ross T, Modesti V, Lorenzin M, Campana C, Punzi L: Erosive hand osteoarthritis and systemic sclerosis: a casual association? *Joint Bone Spine.* 2012 Oct;79(5):507-9. doi: 10.1016/j.jbspin.2012.06.006. Epub 2012 Jul 26. PMID: 22840479.
41. Siao-Pin S, Damian L, Muntean LM, Rednic S: Acroosteolysis in systemic sclerosis: an insight into hypoxia-related pathogenesis. *Exp Ther Med.* 2016 Nov;12(5):3459-3463. doi: 10.3892/etm.2016.3782. Epub 2016 Oct 5. PMID: 27882179; PMCID: PMC5103839.

42. Buckley BJ, Ali U, Kelso MJ, Ranson M. The urokinase plasminogen activation system in rheumatoid arthritis: Pathophysiological roles and prospective therapeutic targets. *Curr Drug Targets*. 2019;20(9):970-981. doi: 10.2174/1389450120666181204164140. PMID: 30516104; PMCID: PMC6700755.
43. Pérez-García S, Carrión M, Jimeno R, Ortiz AM, González-Álvaro I, Fernández J, Gomariz RP, Juarranz Y. Urokinase plasminogen activator system in synovial fibroblasts from osteoarthritis patients: modulation by inflammatory mediators and neuropeptides. *J Mol Neurosci*. 2014 Jan;52(1):18-27. doi: 10.1007/s12031-013-0189-z. Epub 2013 Dec 7. PMID: 24318839.
44. Almholt K, Hebsgaard JB, Nansen A, Andersson C, Pass J, Rono B, Thygesen P, Pelzer H, Loftager M, Lund IK, Hoyer-Hansen G, Frisch T, Jensen CH, Otte KS, Soe NH, Bartels EM, Andersen M, Bliddal H, Usher PA: Antibody-mediated neutralization of uPA proteolytic function reduces disease progression in mouse arthritis models. *J Immunol*. 2018 Feb 1;200(3):957-965. doi: 10.4049/jimmunol.1701317. Epub 2017 Dec 27. PMID: 29282305.
45. Butt S, Jeppesen JL, Iversen LV, Fenger M, Eugen-Olsen J, Andersson C, Jacobsen S: Association of soluble urokinase plasminogen activator receptor levels with fibrotic and vascular manifestation in systemic sclerosis. *PLoS One*. 2021 Feb 22;16(2):e0247256. doi: 10.1371/journal.pone.0247256. PMID: 33617568; PMCID: PMC7899346.
46. Baart VM, Houvast RD, de Geus-Oei LF, Quax PHA, Kuppen PJK, Vahrmeijer AL, Sier CFM. Molecular imaging of the urokinase plasminogen activator receptor: opportunities beyond cancer. *EJNMMI Res*. 2020 Jul 28;10(1):87. doi: 10.1186/s13550-020-00673-7. PMID: 32725278; PMCID: PMC7387399.
47. Jin T, Tarkowski A, Carmeliet P, Bokarewa M. Urokinase, a constitutive component of the inflamed synovial fluid, induces arthritis. *Res Ther*. 2003;5(1):R9-R17. doi: 10.1186/ar606. Epub 2002 Oct 17. PMID: 12716448; PMCID: PMC154426.
48. Dabrowska S, Andrzejewska A, Janowski M, Lukomska B: Immunomodulatory and regenerative effects of mesenchymal stem cells and extracellular vesicles: therapeutic outlook for inflammatory and degenerative diseases. *Front Immunol*. 2021 Feb 5;11:591065. doi: 10.3389/fimmu.2020.591065. PMID: 33613514; PMCID: PMC7893976.
49. Li F, Li X, Liu G, Gao C, Li X: Bone marrow mesenchymal stem cells decrease the expression of RANKL in collagen-induced arthritis rats via reducing the levels of IL-22. *J Immunol Res*. 2019 Nov 7;2019:8459281. doi: 10.1155/2019/8459281. PMID: 31828174; PMCID: PMC6885301.
50. Gao J, Zhang G, Xu K, Ma D, Ren L, Fan J, Hou J, Han J, Zhang L: Bone marrow mesenchymal stem cells improve bone erosion in collagen-induced arthritis by inhibiting osteoclasia-related factors and differentiating into chondrocytes. *Stem Cell Res Ther*. 2020 May 7;11(1):171. doi: 10.1186/s13287-020-01684-w. PMID: 32381074; PMCID: PMC7203805.
51. Thalakiriyawa DS, Jayasooriya PR, Dissanayaka WL: Regenerative potential of mesenchymal stem cell-derived extracellular vesicles. *Curr Mol Med*. 2022; 22(2): 98-119. doi: 10.2174/1566524021666210211114453. PMID: 33573555.
52. Lu C, Chen Y, Ke C, Liu R: Mesenchymal stem cell-derived extracellular vesicle: a promising alternative therapy for osteoporosis. *Int J Mol Sci*. 2021 Nov 25;22(23):12750. doi: 10.3390/ijms222312750. PMID: 34884554; PMCID: PMC8657894.
53. Wang Y, Liu J, Yu B, Jin Y, Li J, Ma X, Yu J, Niu J, Liang X: Umbilical cord-derived mesenchymal stem cell conditioned medium reverses neuronal oxidative injury by inhibition of TRPM2 activation and the JNK signaling pathway. *Mol Biol Rep*. 2022 Aug;49(8):7337-7345. doi: 10.1007/s11033-022-07524-9. Epub 2022 May 18. PMID: 35585377; PMCID: PMC9304044.
54. Shang S, Fang Y, Xin W, You H. The Application of Extracellular Vesicles Mediated miRNAs in Osteoarthritis: Current Knowledge and Perspective. *J Inflamm Res*. 2022 Apr 21;15:2583-2599. doi: 10.2147/JIR.S359887. PMID: 35479833; PMCID: PMC9037713.
55. Zhang C, Zhang W, Zhu D, Li Z, Wang Z, Li J, Mei X, Xu W, Cheng K, Zhong B: Nanoparticles functionalized with stem cell secretome and CXCR4-overexpressing endothelial membrane for targeted osteoporosis therapy. *J Nanobiotechnology*. 2022 Jan 15;20(1):35. doi: 10.1186/s12951-021-01231-6. PMID: 35033095; PMCID: PMC8760699.
56. Amsar RM, Wijaya CH, Ana ID, hidajah AC, Notobroto HB, Wungu TDK, Barlian A: Extracellular vesicles: a promising cell-free therapy for cartilage repair. *Future Sci OA*. (2022) 8(2): FSO774. doi: 10.2144/fsoa-2021-0096. PMID: 35070356; PMCID: PMC8765097.
57. Bao C and He C: The role and therapeutic potential of MSC-derived exosomes in osteoarthritis. *Arch Biochem Biophys*. 2021 Oct 15;710:109002. doi: 10.1016/j.abb.2021.109002. Epub 2021 Aug 2. PMID: 34352243.
58. Jin Z, Ren J, Qi S: Human bone mesenchymal stem cells-derived exosomes overexpressing micro RNA-26a-5p alleviate osteoarthritis via down-regulation of PTGS2. *Int Immunopharmacol*. 2020 Jan;78:105946. doi: 10.1016/j.intimp.2019.105946. Epub 2019 Nov 26.

59. Qiu M, Liu D, Fu Q: MiR-129-5P shuttled by human synovial mesenchymal stem cell-derived exosomes relieves IL-1 $\beta$  induced osteoarthritis via targeting HMGB1. *Life Sci.* 2021 Mar 15;269:118987. doi: 10.1016/j.lfs.2020.118987. Epub 2021 Jan 5. PMID: 33417958.
60. Xian Bo S, Chen W, Chang L, Hao Ran Y, Hui Hui G, Ya Kun Z, Wu Kun X, Hai Tao F, Wen Dan C. The Research Progress of Exosomes in Osteoarthritis, With Particular Emphasis on the Therapeutic Effect. *Front Pharmacol.* 2022 Mar 2;13:731756. doi: 10.3389/fphar.2022.731756. PMID: 35308214; PMCID: PMC8924513.
61. Simental-Mendía M, Lozano-Sepúlveda SA, Pérez-Silos V, Fuentes-Mera L, Martínez-Rodríguez HG, Acosta-Olivo CA, Peña-Martínez VM, Vilchez-Cavazos F. Anti inflammatory and anti catabolic effect of non animal stabilized hyaluronic acid and mesenchymal stem cell conditioned medium in an osteoarthritis coculture model. *Mol Med Rep.* 2020 May;21(5):2243-2250. doi: 10.3892/mmr.2020.11004. Epub 2020 Feb 26. PMID: 32323772.
62. Zhou X, Liang H, Hu X, An J, Ding S, Yu S, *et al.*: BMSC-derived exosomes from congenital polydactyly tissue alleviate osteoarthritis by promoting chondrocyte proliferation. *Cell Death Discov.* 6, 142 (2020). <https://doi.org/10.1038/s41420-020-00374-z>
63. He L, He T, Xing J, Zhou Q, Fan L, Liu C, Chen Y, Tian Z, Wu D, Liu B, Rong L: Bone marrow mesenchymal stem cell-derived exosomes protect cartilage damage and relieve knee osteoarthritis pain in a rat model of osteoarthritis. *Stem Cell Res Ther* 11, 276 (2020). <https://doi.org/10.1186/s13287-020-01781-w>
64. Panagopoulos I, PK and Lambrou GI: Bone erosions in rheumatoid arthritis: recent developments in pathogenesis and therapeutic implications. *J Musculoskelet Neuronal Interact.* 2018 Sep 1;18(3):304-319. PMID: 30179207; PMCID: PMC6146189.
65. Li L, Wang Y, Yu X *et al.* Bone marrow mesenchymal stem cell-derived exosomes promote plasminogen activator inhibitor 1 expression in vascular cells in the local microenvironment during rabbit osteonecrosis of the femoral head. *Stem Cell Res Ther* 11, 480 (2020). <https://doi.org/10.1186/s13287-020-01991-2>
66. Rabieian R, Boshtam M, Zareei M, Kouhpayeh S, Masoudifar A, Mirzaei H. Plasminogen activator inhibitor type-1 as a regulator of fibrosis. *J Cell Biochem.* 2018 Jan;119(1):17-27. doi: 10.1002/jcb.26146. Epub 2017 Jun 12. PMID: 28520219.

## الملخص العربي

## الخلايا الجذعية الميزنشيمية مقابل الوسط المكيف لها لعلاج نموذج إتهاب المفاصل المصاحب للتصلب الجهازى للجرذ: دراسة نسيجية وهستوكيميائية مناعية

أميرة عدلى كساب<sup>١،٢</sup>، أحمد على أحمد عبد الحافظ<sup>٣</sup>، على الديب<sup>٤</sup>، أمل على أحمد عبد الحافظ<sup>١</sup>

<sup>١</sup>قسم الهستولوجيا، كلية الطب، جامعة طنطا، مصر

<sup>٢</sup>قسم العلوم الطبية الأساسية، كلية الطب، جامعة ابن سينا للعلوم الطبية، عمان، الأردن

<sup>٣</sup>قسم التخدير والعناية المركزة وعلاج الألم، كلية الطب، جامعة طنطا، مصر

<sup>٤</sup>قسم الطب الطبيعي والتأهيل، جامعة طنطا، مصر

**المقدمة:** التصلب الجهازى (SS) هو اضطراب في المناعة الذاتية مع ارتفاع معدلات الاعتلال. يتميز بالتهاب وتليف مزمن. تم الإبلاغ عن المظاهر المفصلية لـ SS في العديد من الحالات.

**الهدف من البحث:** استكشاف آليات جديدة تشارك في التصلب الجهازى المرتبط بالتهاب المفاصل ومقارنة التأثيرات العلاجية للخلايا الجذعية الميزنشيمية (BM-MS) والوسط المكيف لها (MS-C) على التهاب مفاصل الركبة المرتبط بنموذج التصلب الجهازى في الجرذان.

**مواد وطرق البحث:** تم تقسيم أربعين جرذاً إلى المجموعة ١ (ضابطة) و المجموعة ٢ (مجموعة التهاب المفاصل المرتبط بـ SS) والمجموعة ٣ (المجموعة المعالجة). وبعد ذلك تم تقسيم المجموعة ٣ إلى المجموعة الفرعية ٣أ (المجموعة المعالجة بـ BM-MS) والمجموعة الفرعية ٣ب (المجموعة المعالجة بـ MS-C) (بعد أربعة أسابيع من آخر حقنة في جميع المجموعات الفرعية، تم إجراء استئصال كامل لمفاصل الركبة لتتم معالجتها من أجل الدراسة النسيجية والكيميائية المناعية).

**النتائج:** كشفت المجموعة ٢ عن خلل في التركيب النسيجي لكل من الغضروف المفصلي وعظم تحت الغضروف والغشاء الزليلي. لوحظ عدم انتظام السطح وشقوق و تآكل سطحي للغضروف. لوحظ تآكل مصفوفة العظام تحت الغضروفية. أظهر الغشاء الزليلي احتقان الأوعية الدموية وذمة وتسلل خلوي التهابي. علاوة على ذلك، كان هناك انخفاض ذا دلالة إحصائية في سمك الغضروف المفصلي وعظم تحت الغضروف وانخفاض محتوى الكولاجين في مصفوفة الغضروف المفصلي. أظهر الغشاء الزليلي ترسب الكولاجين دون الحد الأدنى لطبقة السبنتيما وزيادة لها دلالة إحصائية في التعبير المناعي لمنشط اليوروكيناز البلازمينوجين (UPA). في المقابل، أظهرت المجموعة ٣ تحسناً ملحوظاً في جميع المعلمات المذكورة أعلاه الذي كان ملحوظاً للغاية في المجموعة الفرعية ٣ب مقارنةً بالمجموعة الفرعية ٣أ.

**الإستنتاج:** MS-C له تأثيرات علاجية أفضل من BM-MS على التهاب مفصل الركبة المرتبط بـ SS.